

# Geometrical Configuration of Cabling as Factor Influencing the Reproducibility of EMC Immunity Tests

Jozef HALLON, Karol KOVÁČ, Imrich SZOLIK

Dept. of Measurement, Slovak University of Technology, Ilkovičova 3, 812 19 Bratislava, Slovak Republic

jozef.hallon@stuba.sk, karol.kovac@stuba.sk, imrich.szolik@stuba.sk

**Abstract.** *The paper deals with analysis of the influence of geometrical configuration of device cabling upon voltages induced in cable interfaces. The analyzed properties are the cable height and the cable length for common mode disturbance, and the loop width for differential mode disturbance. The analysis is solved both by analytical calculation and by numerical simulation. Achieved results are compared mutually as well as with results obtained by measurements performed according to standardized procedures. Finally the analyzed parameters are ordered in correspondence of their importance for objectivity and reproducibility of immunity tests against electromagnetic field.*

## Keywords

Electromagnetic compatibility, immunity testing, multiple transmission lines, influence of electromagnetic field, numerical EM simulation.

## 1. Introduction

The aim of this paper is to examine the influence of cabling arrangement changes on frequency dependence of induced currents in device cabling and then on objectivity of immunity test against RF electromagnetic field. The study is based on theoretical analysis of influences of electromagnetic field (EM) on multiple transmission lines (MTL).

Physical consequences to cable lines placed in EM field are described in several literature works. Their aim is to determine the currents flowing along cable interface due to EM field. Nowadays during the period of easy access to relatively powerful computer technology the possibility of usage of some numerical simulation aid for desired analysis is often offered. The advantage of simulation approach is in ability to simply overcome problems with analytical solution for tasks more complicated than textbook examples. In the paper we show also the comparison of analytical, simulation and measured results.

## 2. Theoretical Description of Cable Interfaces Behavior in EM Field

The effects of EM field on transmission lines were published by many authors. We use as a base the theory elaborated by Paul [1], [2], which is until now used and cited by research community as a basement for solving MTL equations. Their aim is the estimation of currents flowing across impedances at the beginning and the end of the cable.

Let us have cabling consisting of  $n$  conductors and one common reference conductor placed in EM field. From integral Faraday law and electric current continuity equation one may derive basic MTL equations:

$$\frac{\partial}{\partial z} \mathbf{V}(z, t) + \mathbf{R}\mathbf{I}(z, t) + \mathbf{L} \frac{\partial}{\partial t} \mathbf{I}(z, t) = \mathbf{V}_F(z, t) \quad (1a)$$

$$\frac{\partial}{\partial z} \mathbf{I}(z, t) + \mathbf{G}\mathbf{V}(z, t) + \mathbf{C} \frac{\partial}{\partial t} \mathbf{V}(z, t) = \mathbf{I}_F(z, t) \quad (1b)$$

where  $\mathbf{L}$ ,  $\mathbf{C}$ ,  $\mathbf{R}$ ,  $\mathbf{G}$  are  $n \times n$  matrices of per-unit-length inductance  $\mathbf{L}$ , capacitance  $\mathbf{C}$ , resistance  $\mathbf{R}$  and conductance  $\mathbf{G}$  of MTL configuration, matrices  $\mathbf{V}(z, t)$  and  $\mathbf{I}(z, t)$  are line voltages and currents, right side matrices  $\mathbf{V}_F(z, t)$  and  $\mathbf{I}_F(z, t)$  contain the effect of the incident field,  $t$  is time variable and  $z$  is longitudinal coordinate.

$\mathbf{R}$  matrix has elements  $(r_i + r_0)$  in its diagonal, all other elements have the value of  $r_0$ , where  $r_0$  is the resistance of the common conductor and  $r_i$  are the resistances of separate wires. Similarly in  $\mathbf{L}$  matrix  $l_{ii}$  elements are intrinsic inductances of separate wires and  $l_{ij}$  constitute mutual inductances between the  $i$ -th and  $j$ -th wire. In  $\mathbf{C}$  matrix  $c_{ii}$  elements correspond to the capacity between the  $i$ -th and the common wire and  $c_{ij}$  constitute negative capacities between the  $i$ -th and  $j$ -th wire. Finally in  $\mathbf{G}$  matrix  $g_{ii}$  elements correspond to the conductivity between the  $i$ -th and the common wire and  $g_{ij}$  constitute negative conductivities between the  $i$ -th and  $j$ -th wire.

Using Thevenin theorem we may express voltages at the beginning and the end of transmission line by formulas:

$$\begin{aligned} \mathbf{V}(0, t) &= -\mathbf{Z}_S \cdot \mathbf{I}(0, t) \\ \mathbf{V}(L, t) &= \mathbf{Z}_L \cdot \mathbf{I}(L, t) \end{aligned} \quad (2)$$

where  $\mathbf{Z}_S$  and  $\mathbf{Z}_L$  are matrices of input and output resistances (general impedances), 0 represents the beginning and  $L$  the end of MTL.

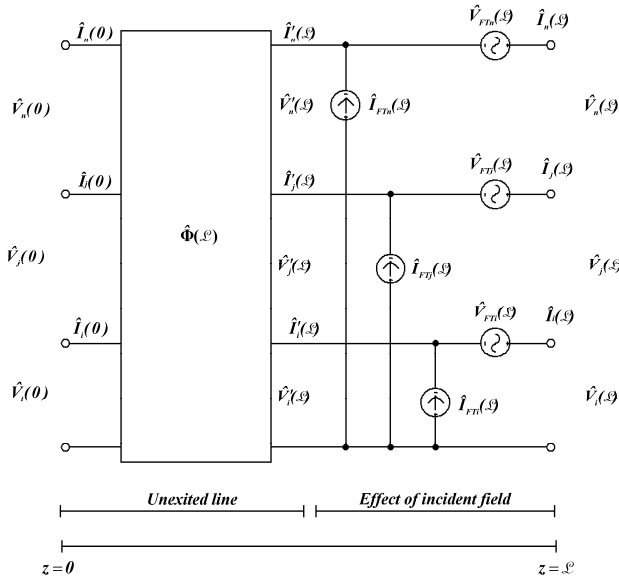


**Fig. 1.** Substitution of multiple transmission line in EM field by parametric matrix and substituting voltage and current sources.

From the point of view of our interest the behavior of MTL in frequency domain is important. Then we may rewrite MTL equations (1a, b) into phasor form. Properties of MTL unexcited by EM field are expressed equivalently by the parametric matrix  $\Phi$  and the influence of EM field is represented by substituting voltage and current sources (Fig. 1). In case when the transmission line is inhomogeneous, it may be composed from a cascade of partial transmission lines, each one having its own parametric matrix [3]. By this way one may also replace cable connection consisting of twisted pair or coaxial cable with unmatched terminal (with pigtailed).

For simplification in further analysis we shall suppose ideal lossless line (this is valid for most of the short lines, which interest us) placed in homogeneous space. Then we shall suppose line excitement by normalized plane EM wave. From general MTL line we shall turn to pair line, where matrices pass to complex scalar variables. This way we obtain sufficiently simple mathematical expressions.

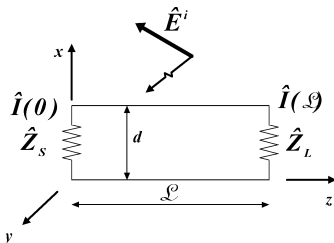


**Fig. 2.** Schematics of two wires symmetrical line.

Relation for the current at the beginning of two wire symmetrical line loaded by impedances  $Z_S$  and  $Z_L$  (Fig. 2) is:

$$\hat{I}(0) = \frac{d\hat{E}_0}{\hat{D}} e^{-j\beta_x d/2} \left[ \frac{\sin\left(\frac{\beta_x d}{2}\right)}{\frac{\beta_x d}{2}} \right] \times \left\{ -j\beta_x e_z \int_0^L \left[ \cosh(\gamma(L-\tau)) + \sinh(\gamma(L-\tau)) \frac{\hat{Z}_L}{\hat{Z}_C} \right] e^{-j\beta_z \tau} d\tau + e_x \left[ \cosh(\gamma L) + \sinh(\gamma L) \frac{\hat{Z}_L}{\hat{Z}_C} - e^{-j\beta_z L} \right] \right\} \quad (3)$$

$$\text{where } \hat{D} = \cosh(\gamma L) (\hat{Z}_S + \hat{Z}_L) + \sinh(\gamma L) \left( \hat{Z}_C + \frac{\hat{Z}_S \hat{Z}_L}{\hat{Z}_C} \right)$$

The line has the width  $d$  oriented in  $x$ -axis direction and the length  $L$  in  $z$ -axis direction. Exciting field is constituted by normalized EM plane wave represented by the intensity  $E_0$  and three corresponding angles respectively by corresponding field intensity components  $e_x, e_y, e_z$ .  $\beta$  is phase constant  $\beta = \omega \sqrt{\mu \epsilon}$ , while  $\beta_x, \beta_y, \beta_z$  are its corresponding components.  $Z_c$  is the characteristic impedance of the line.

The drawing of single wire line ended by impedances  $Z_S$  and  $Z_L$  above infinite perfectly conducting plane is shown in Fig. 3. Line height  $h$  is oriented in  $x$ -axis direction and line length  $l$  is oriented in  $z$ -direction. In this case the problem has to be solved by using the principle of mirroring. Mathematical expression of the current at the beginning is identical with formula (3) under the condition  $d = 2h$ .

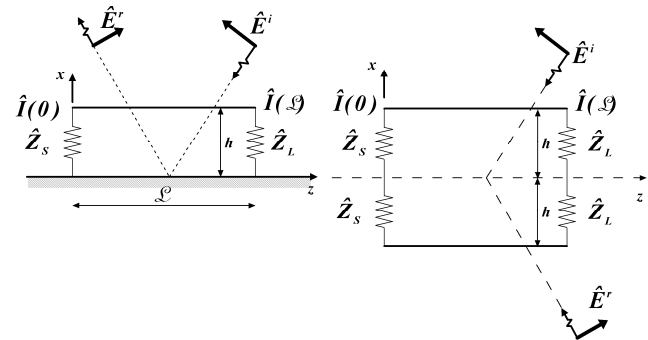


**Fig. 3.** Drawing of single wire line above conducting plane.

It is evident, that the presented theory is applicable first of all for simple textbook examples in homogeneous space and excited by normalized plane EM wave. To achieve reasonably complicated mathematical formulation congruent simplifications are used. For lines with more complicated shape in non-homogeneous space these may cause significant errors. For this reason it is more suitable to use numerical simulation tool to find out the MTL solution. Next limiting property of the mentioned theory is satisfaction of the condition that the maximum dimension of the line arrangement must be sufficiently smaller than the wavelength of external EM field. That makes a limit for line loop dimensions or an upper limit of problem frequency range.

Lines together with loading impedances create loops. In EMC area we distinguish between differential and common loops. They both act simultaneously. In the differential loop differential voltage is generated between two similar wires connected via real impedances. In the common loop common voltage is risen up between separate wires and common reference conductor. Due to larger dimensions common loops are more dangerous for devices with large cable distribution. Similarly by capacitive and inductive undesired coupling the character of disturbance is very often common mode. The current flowing along the line is influenced both by parameters of incident EM wave and by parameters of transmission line and surrounding space.

By appropriate construction of electronic device and relevant cabling one can minimize differential disturbing signal. On the other hand common mode component creates larger problems. Its elimination may be achieved by perfect impedance balancing of a cable interface. This is not a simple problem, because the balance must be achieved in a wide frequency range and not only along the transmission line, but also at terminating impedances. By a balance corruption differential disturbing signal is created, which passes to inputs or other interfaces of electronic circuits.

### 3. Creation of Suitable Simulation Models

Nowadays at our laboratory we use the program system FEKO for numerical simulation. The program FEKO is based on the Method of Moments (MoM). Electromagnetic fields are obtained by calculating the electric surface currents on conducting surfaces firstly and then equivalent electric and magnetic surface currents on the surface of a dielectric solid. The currents are calculated using a linear combination of basis functions, where the coefficients are obtained by solving a system of linear equations. Once the current distribution is known, further parameters can be obtained e.g. the near field, the far field, radar cross sections, directivity or the input impedance of antennas. Electrically large problems are usually solved with either the Physical Optics (PO) approximation and its extensions or the Uniform Theory of Diffraction (UTD). In FEKO these formulations are hybridized with the MoM at the level of the interaction matrix. This is a major step in addressing the problem of solving electromagnetic fields where the object under consideration is too large (in terms of wavelengths) for the MoM, but too small for the asymptotic UTD approximation with high accuracy. With the hybrid MoM/PO or hybrid MoM/UTD techniques, critical regions of the structure can be considered using the MoM and the remaining regions (usually larger, flat or curved metallic surfaces) using the PO approximation or UTD.

The implementation of MoM within FEKO allows us to work with wire, planar and even volumetric segments,

while all segments can have their own complex impedance. It also allows various types of energy excitation.

In our particular case we suffice with quite simple models for modeling of impact of EM field on cable structures. Since we need to model in a relatively wide frequency range, the duration of simulation takes significantly long time (tens of hours on two processors station). So it is important to choose reasonably the length of segments, not too large in comparison with wavelength and not too small, otherwise the time of simulation could rise excessively. Similarly it is reasonable to choose the set of parameters of lines and EM field, which will be modified within simulation process, not to saturate ourselves by quantity of simulation results with small expressing value.

Basic division of models is into:

- Transmission Line with differential mode loop, which model is shown in Fig. 4. The conducting loop consists of larger number of segments, which have precisely defined position in rectangular coordinate system. At the ends of the line, there are impedances with defined values and dimensions. Dimensions of the loop as well as its position may be changed within the model as desired. The loop itself and each loading impedance are placed in separate layer. The simulation current output point is fixed. This allows changing the values of both loading impedances independently, as each may be established by serial combination of electrical resistance, capacitance and inductance. In the defined distance under the loop a dielectric board may be placed constituting the supporting measurement table. As its physical properties affect the propagation of EM wave in its close proximity and consequently the values of induced currents, its relative permittivity and loss coefficient  $\tan \delta$  must be given.

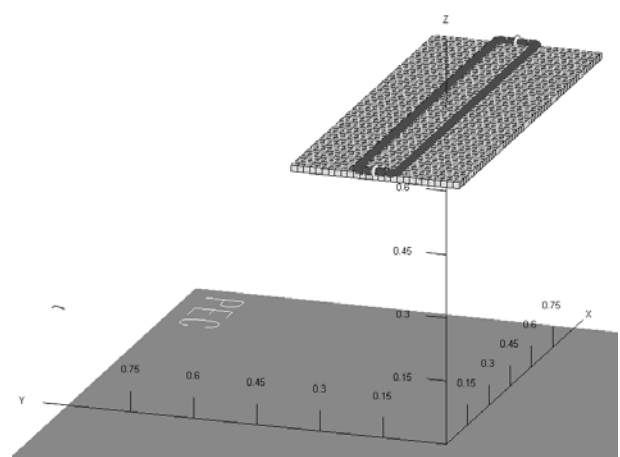


Fig. 4. Simulation model of transmission line with differential loop

Moreover the perfectly conducting plane corresponding to the conducting floor of the measuring place is situated in the defined distance. Finally the

source of excitation has to be specified – linearly polarized plane wave with the given intensity, polarization and direction of propagation. The last parameter is chosen to correspond with the incident wave from the antenna placed in the 3 m distance and height of 1.55 m, what conforms to the real configuration by EMC immunity tests.

- Transmission line with common mode loop is schematically shown in Fig. 5. Similarly to the previous case the conducting loop consists of larger number of segments with the precisely specified position in the model coordinate system. Loading impedances are situated at both line ends. The only difference is, that these impedances are connected to the perfectly conductive plane representing the conductive floor of the measuring place. Under the upper loop the dielectric board is situated as in the previous model. The source of excitation is also the same, but the incident angle must be modified according to the height of the loop wire above the reference plane.

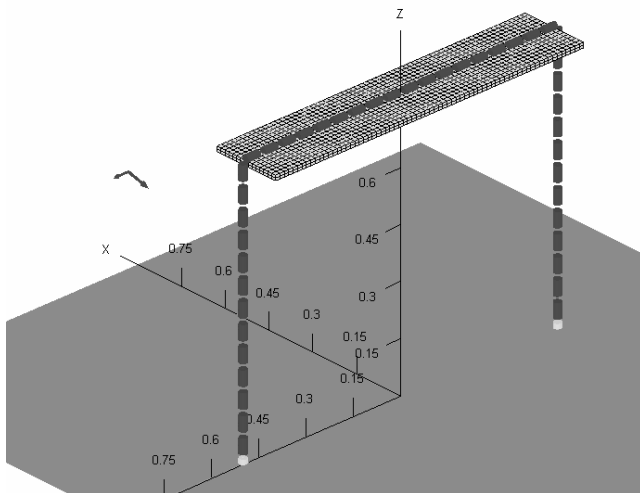


Fig. 5: Simulation model of transmission line with common loop

### 3.1 Comparison of Analytic and Numerical Results

The analytic solution is based upon the theory presented in chapter 2. Graphical representations of frequency dependence of currents flowing along cable wires were obtained by the mathematical program. In the first case we analyzed the transmission line with common loop terminated by real  $50 \Omega$  impedance connected to the floor conductive plane at both ends.

Within the following examples the field was excited by horizontally polarized plane wave with the intensity of  $10 \text{ V/m}$  incident under the angle of  $76^\circ$ . The line length was 1 m and the height above the reference plane was 0.1, 0.4 and 0.8 m. For comparison the calculated and numerically simulated frequency spectra are shown in transparent form in Fig. 6.

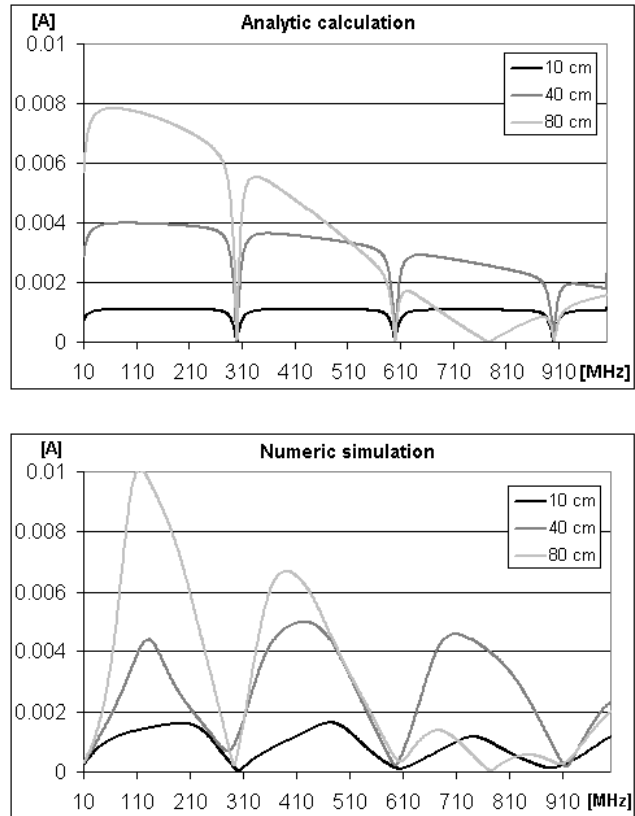


Fig. 6. Calculated and numerically simulated frequency spectra of currents flowing along common mode loop wire for three wire heights.

The measurement was performed in a semi-anechoic shielding chamber. The configuration of measuring places depends on the type of a measured loop. In the case of common mode loop the situation is simpler, because the loading impedance is connected to the reference plane with zero potential. The loading impedance is represented by the 20 dB attenuator. Its output signal was transferred by a coaxial cable to a spectrum analyzer outside of the chamber. At the opposite end of the loop there was the  $50 \Omega$  terminator. The flowing current is proportional to the measured voltage on the terminating impedance [4].

In the case of differential loop the different realization was used. Due to the absence of the reference potential along the loop it was necessary to build the measuring circuit fully symmetrical. Only by this we could obtain the differential component of the loop current. Usually the RF currents are measured by current probes [5], [6], but in our experiment this is not appropriate, because the probe with the output coaxial cable becomes the part of the measuring object arrangement. With their conducting bodies the probe and the cable change the field homogeneity. So we had to build a special measuring circuit for differential voltage measurement. After some unlucky experiments with a passive diode detector we succeeded with the measuring circuit equipped by AD9307 logarithmic amplifier [7]. This circuit has fully symmetrical input, the frequency range from DC up to 500 MHz (with a lower linearity even up to 1 GHz) and the dynamical range of 92 dB. The output

signal was connected to sigma-delta AD converter and by the help of a micro-controller it was transferred outside of the measuring chamber via an optical transmission line.

EM field was generated, the measuring place was calibrated and the measurement was performed according to EN 61000-4-3 standard [8]. It means, that electric component of field was 10 V/m, the frequency step was 1 % of the adjusted frequency within the range from 80 MHz to 480 MHz. We performed the measurement in the range up to 480 MHz only, because we know from our EMC testing experience that the most of equipment failures during testing are in this frequency range. The antenna distance is 3 m in accordance to the standard. VULB 9161 BiConLog antenna was placed in the height of 155 cm above the reference plane. The results presented further were measured under horizontal polarization.

#### 4. Measured and Simulated Results and Their Interpretation

By the analysis of the influence of geometric configuration we concentrated our attention first of all to:

1. the influence of the cable height above the reference plane for common mode loop,
2. the influence of the cable length for common mode loop, and
3. the influence of the loop width within differential loop.

The analysis of the influence of the cable height above the reference plane was performed for common mode loop 1 m long. This problem is significant mainly for sizeable devices, where it is impossible to arrange the cabling according to standardized configuration – in the height of 80 cm upon a wooden table. The effective loop area increases with the rising cabling height, which results in growing of common mode current flowing along the cable. In Fig. 7 one can see the measured and simulated frequency dependence of the voltage at 50  $\Omega$  terminating impedance for the two values of cable height. From the point of view of immunity testing the most important is the maximum voltage peak value. Mainly its amplitude and to a certain extent also the frequency is the terminative parameter for the estimation of sensitivity of the given configuration to EM field. The experience from a testing praxis implies that a decrease of the induced voltage on cables by several dB often has cardinal influence on a correct operation of electronics due to a nonlinear character of semiconductor elements. If the test configuration change results in decreasing of the induced signals upon cabling, it has the influence upon objectivity and reproducibility of the immunity against radiated EM field test. In praxis this problem can be more important. By standard, homogeneity of EM field is guaranteed only in the limited space of 1.5 x 1.5 m area. The lower margin of it is in the height of 0.8 m.

Even in this limited space the homogeneity should be in the range of 6 dB and it is restricted by the calibration standard process and properties of the testing semi-anechoic chamber often with relatively small dimensions. Lower measured values at higher frequencies in comparison with simulated results may be caused by lower intensity of EM field below the specified calibrated test area. This fact was approved by the measurement with the E-field probe sensor in the space under the bottom margin of the standard test area [9]. The intensity of the field falls down to the level of 3 V/m. Ripples in measured spectra are due to the combination of the narrow bandwidth of the measuring spectrum analyzer and the rising frequency step of adjusted EM field.

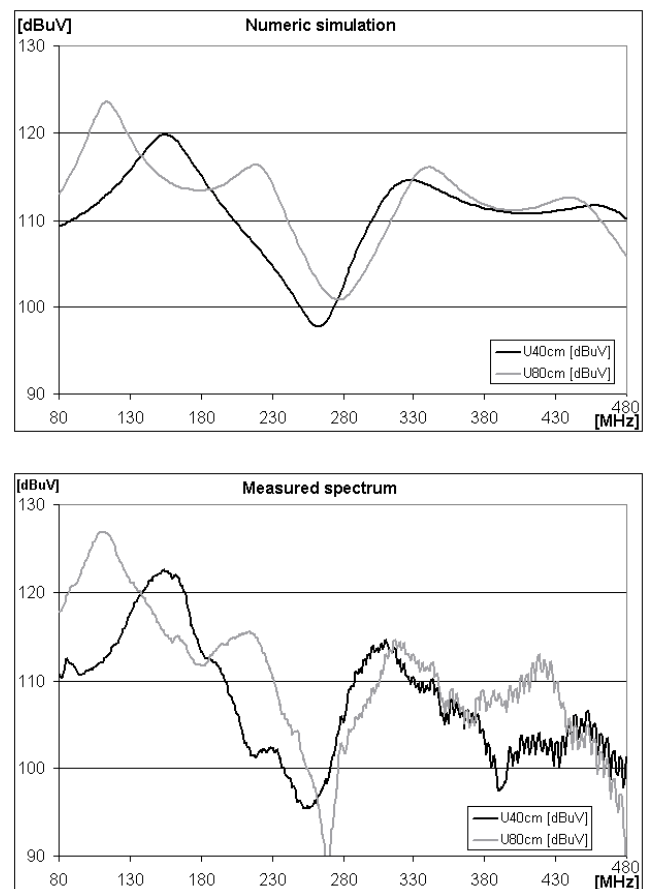
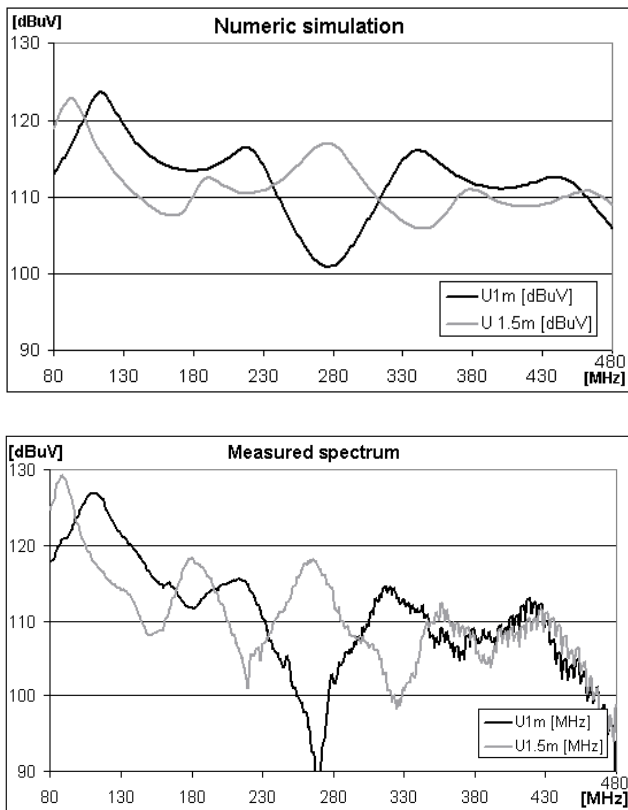


Fig. 7. Simulated and measured frequency dependence of induced voltage on 50  $\Omega$  terminating impedance of common mode loop for two cable heights above reference plane – 40 and 80 cm.

The analysis of the influence of the cable length for common mode loop was performed for cables placed in the height of 80 cm. By large devices it is not possible for various reasons to ensure the reference length of cables (1 m) during immunity tests. Similarly as in the previous case this can cause the change of induced current and voltage amplitudes and then affect the objectivity of the test.

In Fig. 8 one can see the simulated and measured frequency dependence on 50  $\Omega$  terminating impedance for the two cable lengths – 1 m and 1.5 m. A longer cable cannot

be measured due to the limited measuring space area with the guaranteed field homogeneity. We can consider that the presented spectra are in a good agreement despite the limitation of field homogeneity, which was already mentioned. We may conclude that the influence of the cable length is weaker than the influence of the cable height, as small changes in the cable length do not have a significant effect upon the level of the induced voltage. So it is not necessary to keep the cable length as stringent as the height during immunity tests. The simulations performed up to 2.5 m long cables showed only a moderate frequency shift of the main peak of induced currents and corresponding voltages.



**Fig. 8.** Simulated and measured frequency dependence of induced voltage on  $50\ \Omega$  terminating impedance of common mode loop for two cable lengths – 1 and 1.5 m.

The analysis of the influence of the width of differential mode loop was performed for 1 m long lines placed in 80 cm height above the reference plane. By a particular group of devices differential loops created by a cabling system may have influence upon the results of the tests. In Fig. 9 we show the simulated and measured frequency dependence of induced voltages on  $50\ \Omega$  terminating impedance for the four loop widths – 1, 5, 10 and 25 cm. It is evident that this parameter has the major influence on the amplitude of the induced voltage. So it is apparent that the cables of each circuit have to be placed in close proximity to each other. In real installations the cables have to be installed similarly. On the other side the cabling of different circuits has to be separated during the immunity test to

ensure that one group of cables does not shield the field for other cable group.

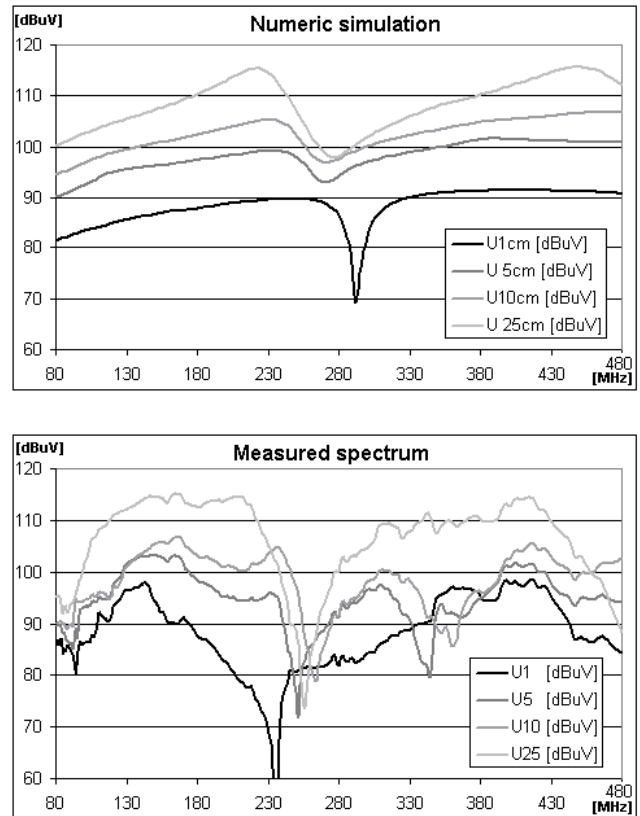


**Fig. 9.** Simulated and measured frequency dependence of induced voltage on  $50\ \Omega$  terminating impedance of differential mode loop for four loop width – 1, 5, 10 and 25 cm.

## 5. Conclusions

The presented results show that the parameters of the geometrical configuration of the device cabling (the cable height and length for common mode loop, and the width of differential mode loop) may have significant influence upon the voltage induced by EM field on the cable interfaces. So it is necessary to pay attention to the positioning of device cables for immunity tests against high frequency EM field. If the position of cables does not correspond with the specified standard configuration the result of the test may not agree with the result under the reference conditions – the test may not be considered as objective. This deduction is even more important by post installation tests of large systems. For these devices due to large dimensions, high power consumption or system complexity it is not possible to keep the standardized procedure in term of neither testing place nor test practice, whether.

It was shown that the most important parameter is the width of differential mode loop (the distance between opposite wires of the loop), less important is the cable height above the reference conductive plane and the least influence has the cable length.

## Acknowledgements

The work presented in this paper was supported by the Slovak Ministry of Education under grant No. 2003SP200280802 and by the Slovak Grant Agency VEGA under grant No. VEGA 1/3101/06.

## References

- [1] PAUL, C. R. A SPICE model for multiconductor transmission lines excited by an incident electromagnetic field. *IEEE Transactions on Electromagnetic Compatibility*. 1994, vol. 36, no. 4, pp. 342 – 354.
- [2] PAUL, C. R. *Analysis of Multiconductor Transmission Lines*. New York: Wiley Interscience, 1994.
- [3] OMID, M., KAMI, Y., HAYAKAWA, M. Field coupling to nonuniform and uniform transmission lines. *IEEE Transactions on Electromagnetic Compatibility*. 1997, vol. 39, no. 3, pp. 201 - 211.
- [4] HALLON, J., BITTERA, M., KOVÁČ, K., SZOLIK, I. Influence of cables position upon repeatability of induced voltages during EMC immunity tests of large systems. In *Proceedings of the XVth International Conference on Electromagnetic Disturbances, EMD 2005*. Białystok (Poland), September 2005, pp. 3.3-1 - 3.3-4.
- [5] SPADACINI, G., PIGNARI, S. A. A bulk current injection test conforming to statistical properties of radiation-induced effects. *IEEE Transactions on Electromagnetic Compatibility*. 2004, vol. 46, no. 3, pp. 446 - 458.
- [6] ADAMS, J. W., CRUZ, J., MELQUIST, D. Comparison measurements of currents induced by radiation and injection. *IEEE Transactions on Electromagnetic Compatibility*. 1992, vol. 34, no. 3, pp. 360 - 362.
- [7] Low Cost DC–500 MHz, 92 dB Logarithmic Amplifier AD 8307. *Datasheet*, Analog Devices, Inc., www.analog.com, 2003.
- [8] *EN 61000-4-3 Electromagnetic compatibility (EMC) - Part 4-3: Testing and measurement techniques - Radiated, radio-frequency, electromagnetic field immunity test*.

- [9] BITTERA, M., HARŤANSKÝ, R. Electromagnetic compatibility EM field measurement. In *Proceedings of the 8th International Symposium on Mechatronics MECHATRONIKA 2005*. Trenčianske Teplice (Slovakia), May 2005, pp. 84 - 87.

## About Authors...

**Jozef HALLON** (Ing., \*1963) graduated in microelectronics from the Faculty of Electrical Engineering, Slovak Technical University of Bratislava in 1987. During the years 1987 - 1992 he worked as a research worker at the Slovak Academy of Science. Since 1992 he has been working as a research worker at the Faculty of Electrical Engineering at the EMC group of the Dept. of Measurement.

**Karol KOVÁČ** (Assoc. Prof., Ing., PhD., \*1952) received the MSc. degree with honors in 1976 and the PhD degree in electrical engineering from the Faculty of Electrical Engineering, Slovak Technical University, Bratislava. Since 1976 he has been with the Dept. of Measurement of the Faculty of Electrical Engineering and Information Technology, Slovak University of Technology, now as Associate professor for Electric Measurement. His research interests are in the area of numerical simulation of EMC phenomena and processes.

**Imrich SZOLIK** (Ing., \*1974) received the M.S degree in electrical engineering from the Faculty of Electrical Engineering and Information Technology, Bratislava, Slovakia in 1999. He is working as researcher at the Faculty of Electrical Engineering and Information Technology, Bratislava, Slovakia. His research interests are in automated instrumentation, digital signal processing, numerical simulation and information technologies.

## MOW Conference Week 14 to 18 May, 2007, Budapest, Hungary

- *Submission of 4 pages full paper: 20 January, 2007* • *Notification of acceptance: 10 March, 2007* •

**MMS2007** • Wave propagation, scattering, diffraction • Antenna theory and applications • Electromagnetic field analysis • Inverse scattering and diagnostics • Waves in composite and complex media • Photonics, non-linear optics and devices • Medical applications, bio-electromagnetic modeling • Electromagnetic compatibility • Microwave and millimeter-wave devices • Passive microwave components and technologies • RF and wireless technology and applications • Packaging, integration and testing

**MICROCOLL** • Mobile cellular urban and rural communications • Wireless access networks • Indoor wireless and optical systems • Satellite mobile and fix optical systems • Terrestrial microwave radio links • Combined wireless and optical systems • Wireless antennas and propagation • Microwave and optical electronics • Microwave and optical integrated circuits (monolithic and hybrid) • Microwave and optical measurements • CAD for RF/microwave/optical circuits and subsystems • Biological effects of microwave and optical radiation • Industrial applications

**[www.diamond-congress.hu/mow2007](http://www.diamond-congress.hu/mow2007)**